High-Conversion Diffusion-Controlled Copolymerization Kinetics

D. K. Sharma† and D. S. Soane* (Soong)

Department of Chemical Engineering, University of California, Berkeley, California 94720. *Received April 27, 1987; Revised Manuscript Received September 25, 1987*

ABSTRACT: Simultaneous polymerization of two or more monomers is a commercially important process for tailor making polymer properties. A major problem with this technique, however, is the well-known copolymer composition drift resulting from reactivity differences between the component monomers. During the course of copolymerization, the product formed becomes progressively depleted in the faster reacting monomer, a situation very similar to that occurring in Rayleigh semibatch distillation. In addition to intrinsic reactivity differences, diffusional processes exert a strong influence on the instantaneous molecular weight and possibly on the copolymer composition produced, especially toward higher levels of conversion. Proper consideration of diffusion limitations at higher conversions may thus be an integral part of any optimization scheme for controlling composition drift. The purpose of this work is to develop a high-conversion diffusion-controlled copolymerization model to predict the molecular weight and composition evolution. The model incorporates free-volume based diffusion theories of polymers as before in a homopolymerization model for high conversions.

Introduction

As polymer applications continue to diversify, more demands are placed on the engineering of these materials. Part of the demands can be met by synthesizing new monomers. Such resources are rather limited, however, and the number of new polymers has not increased at a pace in keeping with the rising demands of product performance. A better approach is to copolymerize judiciously chosen monomer pairs or even multiple monomer combinations to achieve the desired properties. This idea has stimulated a growing copolymerization industry, making copolymerization an important area of research.

Except for a few special cases of initial monomer compositions, i.e., the azeotropic mixtures, products of a typical free-radical copolymerization show a gradual drift in the copolymer composition over the course of copolymerization. This well-known copolymer composition drift phenomenon stems from the different reactivities of the monomers to combine with the growing polymer radicals. Hence, the more reactive monomer is depleted at first, causing the product to become gradually enriched in the less reactive monomer as reaction progresses. This situation is quite similar to a batch distillation process, where liquid mixture evaporating into the vapor phase is conceptually equivalent to monomer mixture reacting to form the product copolymer. A major difference exists, however, in that the copolymer formed usually resides in the same phase as the monomer mixture (except for cases where the copolymer precipitates from the solution), whereas distillation involves two distinct phases. The gradual buildup of the macromolecule causes an increase in the viscosity of the reacting mixture. Hence, termination as well as propagation steps can both be affected by diffusion limitations. Diffusion-controlled reaction may also lead to both composition and molecular weight drifts. This factor compounds the contributions from the intrinsic monomer reactivity difference. Diffusion-controlled composition and molecular weight drifts can become critical considerations for reactions carried to high conversions.

Before developing the model proposed in this paper to simulate copolymerization to high conversions, we will review the literature on copolymerization with special attention to unsolved problems in this area.

Major developments of the present copolymerization equation were independently made in 1944 by Alfrey and Goldfinger,[1] Mayo and Lewis,[2] and Wall,[3] the validity of which was established by May and Lewis[2] using styrene–methyl methacrylate and repeatedly confirmed by others. Generalization of the copolymer scheme to n-monomers can also be found in the paper by Wall.[3] Skiest[4] showed the analogy between copolymerization and distillation and derived an equation similar to the Raleigh equation, which related vapor composition and yield in distillation (or, equivalently, copolymer composition and conversion in polymerization). This method led to the computation of the composition distribution of copolymers. Mayo and Walling[5] wrote the first review on copolymerization in 1950. It encompassed the theory for composition of copolymers formed in free radical copolymerization, the relation between structure and reactivity of olefin toward hydrocarbon free radicals, and the overall rates of copolymerization. A few studies of copolymerization by an ionic mechanism were also reviewed. *High Polymer Series*, Vol. XVIII,[6] contains the first collection of articles on copolymerization. Meyer and Lowry[7] successfully integrated the Skiest[4] copolymerization equation and obtained an analytical solution for the case of binary copolymerization. Equations were also derived for differential copolymer composition, which permitted the calculation of expected binary copolymerization behavior as a function of conversion.

Hanson and Zimmerman[8] examined the problem of composition drift in copolymerization and proposed continuous recycle to produce predictable and homogeneous composition at relatively high percentage of solids. Their scheme is particularly suited for polymerization at high temperature or high pressure by keeping the viscosity of the circulating polymer manageable. This approach is highly energy intensive, however, and requires conversion per pass to be low.

Hanna[9] suggested a rapid method for computing the amount of monomer to be added to produce a chemically uniform copolymer. His approach allowed calculations for the time rate of addition of the faster reacting monomer. O'Driscoll and Knorr[10] presented an analytical expression which gave conversion as a function of time. Derivation and experimental verification of this equation were presented for the methyl methacrylate/vinyl acetate monomer pair. Multicomponent polymerization rate equations were also described, similar to the binary copolymerization approach.

O'Driscoll and Knorr[11] in a later study examined the effects of mixing on copolymerization in CSTR. Broadening of copolymer composition distribution was expected

* To whom correspondence should be directed.
† Currently with Dow Chemical Co., Midland, MI.

0024-9297/88/2221-0700$01.50/0

from reactions conducted in a batch reactor or CSTR with poor mixing. Their calculations ignored the effect of increasing viscosity on rate constants.

Szabo and Nauman[12] discussed means of predicting composition distribution in copolymers and illustrated the strong influence of segregation in the reactor. Pseudo-first-order, isothermal reaction kinetics were used to simplify actual copolymerization rates. Maximum mixedness was needed to produce constant composition copolymers. A recycle loop reactor was suggested as one alternative to approach maximum mixedness.

Ray and Gall[13] addressed the problem of maintaining a specified copolymer distribution in a batch reactor. The advantages of temperature control, rather than monomer addition, were discussed, and the conditions for temperature control in the presence of monomer depletion were derived. Ray[14] also examined the quasi-steady-state assumption (QSSA), when applied to CSTR and batch reactor. The longer induction period in CSTR resulted in QSSA errors larger than in the batch reactor, but the errors were only significant when the conversion in CSTR was low. An alternative approximation by expanding QSSA as an appropriate singular perturbation was recommended.

Macklenburg[15] studied the influence of mixing on the distribution of copolymer composition. This paper first considered this effect theoretically by using an accepted model of free radical copolymerization and then suggested a method by which copolymerization could be used to study mixing. The treatment ignored chain transfer and gel effects. Plug flow reactors and CSTR would be especially useful for distinguishing molecular and macroscopic mixing.

Tirrell and Gromley[16] studied composition control of free radical batch copolymerization by using optimum temperature versus time, discrete and continuous policies. The discrete version of maximization principle[17] was used to compute discrete policy, and the continuous policy was enforced by manipulating the monomer mass balance. Difficulty in controlling the time–temperature policy in solution polymerization limited experimental success in controlling copolymer composition drift, as the composition was very sensitive to deviation from optimality. Tirrel et al.[18] recently examined the optimal design and control problems of copolymerization in a batch reactor as a multiobjective dynamic optimization problem. Noninferior or Parero sets of optimal solutions have been determined for the dual objective of narrowing both copolymer composition distribution and molecular weight distribution of styrene–acrylonitrile in batch and semibatch copolymerization. Continuous monomer addition was found to be a more effective manipulated variable than temperature for composition distribution narrowing.

Semicontinuous emulsion copolymerization with the aim of producing constant-composition copolymers has been examined by Guyot et al.[19] for styrene–acrylonitrile and by Garcia-Rejon et al.[20] for butyl acrylate–styrene system.

While the integrated form[7] of the standard copolymerization equations[1-3] described well the experimental observations of copolymerization of an 80:20 mixture of styrene–methyl methacrylate (MMA) at 60 °C,[21,22] considerable discrepancy has been noted by Johnson et al.[23] between experimental data and predictions of the integrated copolymer composition equation for bulk reactions with an initial feed composition of either 60% or 35% styrene. Confirmation of this unexpected discrepancy stimulated an experimental study by Dionisio and O'Driscoll.[24] In this paper, the authors recognized that the observed discrepancy could be attributed to the fact that reactivity ratios calculated from the classical model were only apparent ones and lacked the physical significance of being true simple ratios of propagation rate constants at high conversions, as a result of diffusion limitations.

Teramachi et al.[25] prepared high-conversion samples of different starting composition styrene–methyl methacrylate copolymers, and determined the copolymer composition distribution (CCD) by thin-layer chromatography (TLC) method.[26-28] Their data agreed fairly well with the theory of copolymerization,[7] and they therefore concluded that no mass-transfer-limitation affected the propagation rate constants at high conversion. They also showed that the published data of Dionisio and O'Driscoll deviated significantly from the predicted CCD.

O'Driscoll et al.[29] revisited the same subject and acknowledged that their earlier work was in error. New data were published for conversion history and cumulative copolymer composition. Using one set of reactivity ratios: $r_1 = 0.4971$ and $r_2 = 0.4639$, they found adequate fit to the data by the Meyer–Lowry equation.[7] However, the new experimental data covered only up to 70 wt % conversion. Hence, it still leaves the question of copolymer composition drift at higher conversions (glassy state), where monomer mass-transfer limitations may be operative.

Garcia-Rubio et al.[30] undertook an extensive experimental study on the bulk copolymerization of styrene and acrylonitrile. A mathematical model based on a free-volume theory to account for diffusion controlled termination and propagation was developed. The model predictions of conversion, composition, and sequence length development are in reasonable agreement with their data. The composition histories for this monomer pair did not exhibit any of the discrepancies noted by Johnson et al.[23] Jones et al.[31] experimentally investigated the kinetics of methyl methacrylate–*p*-methylstyrene up to high conversions and extended the Marten and Hamielec[32] homopolymerization, free-volume-based model to copolymerization. Again, good agreement of model prediction with the data is obtained. The lack of sufficiently accurate experimental composition data prevented these authors from ascertaining the diffusion limitation on the propagation rate constants. Thus, the reactivity dependence on conversion could not be resolved.

Bhattacharya et al.[33] reported the bulk thermal copolymerization of styrene–*p*-methylstyrene. Their model also followed the same free-volume approach considered in the earlier two papers. The copolymer composition was not reported in this work.

In a previous publication from our group,[34] we derived a mathematical model to describe free radical polymerization reactions exhibiting a strong gel effect (Trommsdorff effect).[35] Diffusion limitation was viewed as an integral part of the chain-termination process from the very beginning of polymerization. Its effect on the overall rate of termination gradually increased with conversion and became dominant around certain conversion levels traditionally associated with the onset of the gel effect. The model also considered the glass effect, which occurred only at high conversions when even monomer diffusion to reactive radical sites was severely curtailed. Thus, this model described the polymerization process over the entire course of reaction. Model prediction agreed well with literature data on conversion history and product molecular weights for isothermal PMMA polymerization. In the present paper, we will extend this basic homopolymerization model to describe copolymerization reactions to high conversions where both the gel and glass effects are important and may contribute significantly to the observed molecular weight

and more importantly composition drifts.

Theory

Copolymerization Reaction Mechanism and Kinetic Equations. In order to keep the analysis as simple as possible the free radical copolymerization reaction mechanism adopted here consists of standard initiation, propagation, and termination steps only. Chain-transfer reactions are neglected for convenience but can be incorporated for systems with known chain-transfer processes.

The detailed mechanism is as follows:

Initiation

$$I \rightarrow 2R \qquad \text{rate} = K_{DI}I$$

$$R + M_i \rightarrow P_{10} \qquad \text{rate} = K_{Ii}M_iR$$

where I is the initiator, R is the primary initiator radical, M_i is the monomer.

Propagation

$$P_{n,m} + M_1 \rightarrow P_{n+1,m} \qquad \text{rate} = K_{p\,11}P_{n,m}M_1$$

$$P_{n,m} + M_2 \rightarrow Q_{n,m+1} \qquad \text{rate} = K_{p\,12}P_{n,m}M_1$$

$$Q_{n,m} + M_1 \rightarrow P_{n+1,m} \qquad \text{rate} = K_{p\,21}Q_{n,m}M_1$$

$$Q_{n,m} + M_2 \rightarrow Q_{n,m+1} \qquad \text{rate} = K_{p\,22}Q_{n,m}M_2$$

where $P_{n,m}$ is a living polymer (concentration = $P_{n,m}$) radical, with n units of M_1 and m units of M_2 and terminal group M_1, while $Q_{n,m}$ is a polymer living radical (concentration = $Q_{n,m}$), with n units of M_1 and m units of M_2 and terminal group m_2.

Termination

Combination

$$P_{n,m} + P_{r,q} \rightarrow M_{n+r,m+q} \qquad \text{rate} = K_{c\,11}P_{n,m}P_{r,q}$$

$$P_{n,m} + Q_{r,q} \rightarrow M_{n+r,m+q} \qquad \text{rate} = K_{c\,12}P_{n,m}Q_{r,q}$$

$$Q_{n,m} + Q_{r,q} \rightarrow M_{n+r,m+q} \qquad \text{rate} = K_{c\,22}Q_{n,m}Q_{r,q}$$

Disproportionation

$$P_{n,m} + P_{r,q} \rightarrow M_{n,m} + M_{r,q} \qquad \text{rate} = K_{d\,11}P_{n,m}P_{r,q}$$

$$P_{n,m} + Q_{r,q} \rightarrow M_{n,m} + M_{r,q} \qquad \text{rate} = K_{d\,12}P_{n,m}Q_{r,q}$$

$$Q_{n,m} + P_{r,q} \rightarrow M_{n,m} + M_{r,q} \qquad \text{rate} = K_{d\,21}Q_{n,m}P_{r,q}$$

$$Q_{n,m} + Q_{r,q} \rightarrow M_{n,m} + M_{r,q} \qquad \text{rate} = K_{d\,22}Q_{n,m}Q_{r,q}$$

where $M_{i,j}$ are the dead polymer with i units of monomer M_1 and j units of monomer M_2 and the K's are relevant rate constants.

For well-stirred batch reactions, mass balance for each species gives the following set of differential equations:

$$\frac{1}{V}\frac{d(IV)}{dt} = -K_{DI}I \tag{1}$$

where V is the system volume,

$$\frac{1}{V}\frac{d(RV)}{dt} = 2fK_{DI}I - (R_1 + R_2) \tag{2}$$

where $0 \le f \le 1$ is an efficiency factor to account for other simultaneous reactions consuming R.

$$\frac{1}{V}\frac{d(M_1V)}{dt} = -R_1 - (K_{p\,11}\alpha + K_{p\,21}\beta)M_1 \tag{3}$$

$$\frac{1}{V}\frac{d(M_2V)}{dt} = -R_2 - (K_{p\,12}\alpha + K_{p\,22}\beta)M_2 \tag{4}$$

where $\alpha = \sum_{n=1}^{\infty}\sum_{m=1}^{\infty}P_{n,m}$ and $\beta = \sum_{n=1}^{\infty}\sum_{m=1}^{\infty}Q_{n,m}$; for $n \ge 1$

$$\frac{1}{V}\frac{d(P_{10}V)}{dt} = R_1 - [K_{p\,11}M_1 + K_{p\,12}M_2 + (K_{c\,11} + K_{d\,11})\alpha + (K_{c\,12} + K_{d\,12})\beta]P_{10} \tag{5}$$

$$\frac{1}{V}\frac{d(Q_{01}V)}{dt} = R_2 - [K_{p\,21}M_1 + K_{p\,22}M_2 + (K_{c\,12} + K_{d\,12})\alpha + (K_{c\,22} + K_{d\,22})\beta]Q_{01} \tag{6}$$

$$\frac{1}{V}\frac{d(P_{n,m}V)}{dt} = [K_{p\,11}P_{n-1,m} + K_{p\,21}Q_{n-1,m}]M_1 - [K_{p\,11}M_1 + K_{p\,12}M_2 + (K_{c\,11} + K_{d\,11})\alpha + (K_{c\,12} + K_{d\,12})\beta]P_{n,m} \tag{7}$$

for $m > 1$

$$\frac{1}{V}\frac{d(Q_{n,m}V)}{dt} = [K_{p\,12}P_{n,m-1} + K_{p\,22}Q_{n,m-1}]M_2 - [K_{p\,21}M_1 + K_{p\,22}M_2 + (K_{c\,12} + K_{d\,12})\alpha + (K_{c\,22} + K_{d\,22})\beta]Q_{n,m} \tag{8}$$

and for n and $m \ge 1$

$$\frac{1}{V}\frac{d(\alpha V)}{dt} = R_1 + K_{p\,21}M_1\beta - K_{p\,12}M_2\alpha - [(K_{c\,11} + K_{d\,11})\alpha + (K_{c\,12} + K_{d\,12})\beta]\alpha \tag{9}$$

$$\frac{1}{V}\frac{d(\beta V)}{dt} = R_2 + K_{p\,12}M_2\alpha - K_{p\,21}M_1\beta - [(K_{c\,12} + K_{d\,12})\alpha + (K_{c\,22} + K_{d\,22})\beta]\beta \tag{10}$$

$$\frac{1}{V}\frac{d(M_{n,m}V)}{dt} = \tfrac{1}{2}K_{c\,11}\sum_{r=0}^{n}\sum_{q=0}^{m}P_{r,q}P_{n-r,m-q} + K_{c\,12}\sum_{r=0}^{n}\sum_{q=0}^{m}P_{r,q}Q_{n-r,m-q} + \tfrac{1}{2}K_{c\,22}\sum_{r=0}^{n}\sum_{q=0}^{m}Q_{r,q}Q_{n-r,m-q} + K_{d\,11}P_{n,m}\alpha + K_{d\,12}(P_{n,m}\beta + Q_{n,m}\alpha) + K_{d\,22}Q_{n,m}\beta \tag{11}$$

Fractional conversion is defined by

$$x = \frac{M_0V_0 - MV}{M_0V_0}$$

where M_0 and V_0 are the total monomer concentration and the total system volume, respectively, at zero conversion.

A linear total system volume contraction is assumed

$$V = V_0(1 + \epsilon x) \tag{12}$$

where ϵ is the volume expansion factor and is equal to $(\bar{d}_m - d_p)/d_p$ and $\bar{d}_m$ and d_p are the average monomer mixture and copolymer density, respectively. We next substitute eq 12 in the definition of conversion to obtain M (total monomer concentration at any time t) and x:

$$M = \frac{M_0(1 - x)}{(1 + \epsilon x)} \tag{13}$$

In order to obtain the average molecular weight of the growing radicals and the dead polymer, we invoke the method of moments as suggested by Ray.[14] The three leading moments are given by

$$\lambda_0 = \sum_{n=1}^{\infty}\sum_{m=1}^{\infty}P_{n,m} \tag{14a}$$

$$\lambda_1 = \sum_{n=1}^{\infty}\sum_{m=1}^{\infty}(nw_1 + mw_2)P_{n,m} \tag{14b}$$

$$\lambda_2 = \sum_{n=1}^{\infty}\sum_{m=1}^{\infty}(nw_1 + mw_2)^2P_{n,m} \tag{14c}$$

λ_0, λ_1, and λ_2 are the zeroth, first, and second moment of the growing radical with terminal group M_1 and nw_1 and mw_2 are the total molecular weight due to monomer 1 and monomer 2. Similarly

$$\zeta_0 = \sum_{n=1}^{\infty}\sum_{m=1}^{\infty} Q_{n,m} \tag{15a}$$

$$\zeta_1 = \sum_{n=1}^{\infty}\sum_{m=1}^{\infty} (nw_1 + mw_2)Q_{n,m} \tag{15b}$$

$$\zeta_2 = \sum_{n=1}^{\infty}\sum_{m=1}^{\infty} (nw_1 + mw_2)^2 Q_{n,m} \tag{15c}$$

ζ_0, ζ_1, and ζ_2 are the zeroth, first, and second moment of the growing radical with terminal group M_2 and finally

$$\mu_k = \sum_{n=1}^{\infty}\sum_{m=1}^{\infty} (nw_1 + mw_2)^k M_{n,m} \tag{16}$$

where μ_k, for $k = 0$, 1, and 2, defines the corresponding zeroth, first, and second moments of a dead polymer.

Considerable algebraic simplicity is achieved if the higher moments of the molecular weight distribution are derived by using the method of *generating functions*. Let E, F, and G be the generating functions of the "live" and "dead" copolymer, defined as

$$E(u_1,u_2,t) = \sum_{n=1}^{\infty}\sum_{m=1}^{\infty} u_1^n u_2^m P_{n,m} \tag{17}$$

$$F(u_1,u_2,t) = \sum_{n=1}^{\infty}\sum_{m=1}^{\infty} u_1^n u_2^m Q_{n,m} \tag{18}$$

$$G(u_1,u_2,t) = \sum_{n=1}^{\infty}\sum_{m=1}^{\infty} u_1^n u_2^m M_{n,m} \tag{19}$$

From the generating function E of the "live" copolymer radical, using the transformation

$$u_1 = su^{w_1} \qquad u_2 = su^{w_2} \tag{20}$$

where u and s are the transformation variables, we obtain

$$E(s,u,t) = \sum_{n=1}^{\infty}\sum_{m=1}^{\infty} s^{n+m} u^{nw_1+mw_2} P_{n,m} \tag{21}$$

Then the three leading moments are derived from eq 21 as follows:

$$\lambda_0 = E(1,1,t) \tag{22a}$$

$$\lambda_1 = \partial E/\partial u|_{s=1,u=1} \tag{22b}$$

$$\lambda_2 = \partial^2 E/\partial u^2|_{s=1,u=1+\lambda_1} \tag{22c}$$

and similarly for F and G.

By multiplying eq 5 and 7 by $u_1^n u_2^m$, summing, and then applying the convolution theorem for the generating function, we obtain

$$dE/dt = I_1u_1 + u_1(K_{p\,11}E + K_{p\,21}F)M_1 - [(K_{p\,11}M_1 + K_{p\,12}M_2) + \lambda_0(K_{c\,11} + K_{d\,11}) + \zeta_0(K_{c\,12} + K_{d\,12})]E \tag{23}$$

$$dF/dt = I_2u_2 + u_2(K_{p\,12}E + K_{p\,22}F)M_2 - [(K_{p\,21}M_1 + K_{p\,22}M_2) + \lambda_0(K_{c\,12} + K_{d\,12}) + \zeta_0(K_{c\,22} + K_{d\,22})]F \tag{24}$$

and similarly, from eq 11, we have

$$dG/dt = \tfrac{1}{2}K_{c\,11}E^2 + K_{c\,12}EF + \tfrac{1}{2}K_{c\,22}F^2 + K_{d\,11}\lambda_0E + K_{d\,12}(\zeta_0E + \lambda_0F) + K_{d\,22}\zeta_0F \tag{25}$$

Applying the transformation eq 20 to eq 23–25 and differentiating both sides of the resulting equations with respect to u, along with the linear volume contraction assumption, give the final equations for model calculations.

$$\frac{dx}{dt} = \frac{(1+\epsilon x)}{M_0}[M_1(K_{p\,11}\lambda_0 + K_{p\,21}\zeta_0) + M_2(K_{p\,12}\lambda_0 + K_{p\,22}\zeta_0) + \epsilon_1K_{p\,11}M_1R + \epsilon_2K_{p\,22}M_2R] \tag{26}$$

$$\frac{dI}{dt} = -K_{DI}I - \frac{\epsilon I}{M_0}[K] \tag{27}$$

where

$$K = M_1(K_{p\,11}\lambda_0 + K_{p\,21}\zeta_0) + M_2(K_{p\,12}\lambda_0 + K_{p\,22}\zeta_0) + \epsilon_1K_{p\,11}M_1R + \epsilon_2K_{p\,22}M_2R \tag{28}$$

$$dR/dt = 2fK_{DI}I - R(\epsilon_1K_{p\,11}M_1 + \epsilon_2K_{p\,22}M_2) \tag{29}$$

$$\frac{dM_1}{dt} = -M_1(K_{p\,11}\lambda_0 + K_{p\,21}\zeta_0) - \frac{\epsilon M_1}{M_0}[K] - \epsilon_1K_{p\,11}M_1R \tag{30}$$

$$\frac{dM_2}{dt} = -M_2(K_{p\,12}\lambda_0 + K_{p\,22}\zeta_0) - \frac{\epsilon M_2}{M_0}[K] - \epsilon_2K_{p\,22}M_2R \tag{31}$$

$$d\lambda_0/dt = -\frac{\epsilon\lambda_0}{M_0}[K] - \lambda_0[(K_{c\,11} + K_{d\,11})\lambda_0 + (K_{c\,12} + K_{d\,12})\zeta_0] - K_{p\,12}M_2\lambda_0 + K_{p\,21}M_1\zeta_0 + \epsilon_1K_{p\,11}M_1R \tag{32}$$

$$\frac{d\lambda_1}{dt} = -\frac{\epsilon\lambda_1}{M_0}[K] - [K_{p\,11}M_1 + K_{p\,12}M_2 + \lambda_0(K_{c\,11} + K_{d\,11}) + \zeta_0(K_{c\,12} + K_{d\,12})]\lambda_1 + M_1(K_{p\,11}\lambda_1 + K_{p\,21}\zeta_1) + M_1w_1[K_{p\,11}\lambda_0 + K_{p\,21}\zeta_0] + \epsilon_1K_{p\,11}M_1w_1R \tag{33}$$

$$\frac{d\lambda_2}{dt} = -\frac{\epsilon\lambda_2}{M_0}[K] - [K_{p\,11}M_1 + K_{p\,12}M_2 + \lambda_0(K_{c\,11} + K_{d\,11}) + \zeta_0(K_{c\,12} + K_{d\,12})](\lambda_2 - \lambda_1) + M_1w_1(w_1 - 1)(K_{p\,11}\lambda_0 + K_{p\,21}\zeta_0) + M_1[K_{p\,11}(\lambda_2 + \lambda_1(2w_1 - 1)) + K_{p\,21}(\zeta_2 + \zeta_1(2w_1 - 1))] + \epsilon_1K_{p\,11}M_1w_1(w_1 - 2)R \tag{34}$$

$$\frac{d\zeta_0}{dt} = -\frac{\epsilon\zeta_0}{M_0}[K] - \zeta_0[(K_{c\,12} + K_{d\,12})\lambda_0 + (K_{c\,22} + K_{d\,22})\zeta_0] + K_{p\,12}M_2\lambda_0 - K_{p\,21}M_1\zeta_0 + \epsilon_2K_{p\,22}M_2R \tag{35}$$

$$\frac{d\zeta_1}{dt} = -\frac{\epsilon\zeta_1}{M_0}[K] - [K_{p\,21}M_1 + K_{p\,22}M_2 + \lambda_0(K_{c\,12} + K_{d\,12}) + \zeta_0(K_{c\,22} + K_{d\,22})]\zeta_1 + M_2(K_{p\,12}\lambda_1 + K_{p\,22}\zeta_1) + M_2w_2[K_{p\,12}\lambda_0 + K_{p\,22}\zeta_0] + \epsilon_2K_{p\,22}M_2w_2R \tag{36}$$

$$\frac{d\zeta_2}{dt} = -\frac{\epsilon\zeta_2}{M_0}[K] - [K_{p\,21}M_1 + K_{p\,22}M_2 + \lambda_0(K_{c\,12} + K_{d\,12}) + \zeta_0(K_{c\,22} + K_{d\,22})](\zeta_2 - \zeta_1) + M_2w_2(w_2 - 1)(K_{p\,22}\zeta_0 + K_{p\,12}\lambda_0) + M_2[K_{p\,12}(\lambda_2 + \lambda_1(2w_2 - 1)) + K_{p\,22}(\zeta_2 + \zeta_1(2w_2 - 1))] + \epsilon_2K_{p\,22}M_2w_2(w_2 - 2)R \tag{37}$$

$$\frac{d\mu_0}{dt} = -\frac{\epsilon\mu_0}{M_0}[K] + [\tfrac{1}{2}K_{c\,11} + K_{d\,11}]\lambda_0^2 + (K_{c\,12} + 2K_{d\,12})\lambda_0\zeta_0 + (\tfrac{1}{2}K_{c\,22} + K_{d\,22})\zeta_0^2 \tag{38}$$

$$\frac{d\mu_1}{dt} = -\frac{\epsilon\mu_1}{M_0}[K] + (K_{c\,11} + K_{d\,11})\lambda_0\lambda_1 + [(K_{c\,12} + K_{d\,12})(\lambda_0\zeta_1 + \lambda_1\zeta_0)] + (K_{c\,22} + K_{d\,22})\zeta_0\zeta_1 \tag{39}$$

$$\frac{d\mu_2}{dt} = -\frac{\epsilon\mu_2}{M_0}[K] + (K_{c\,11} + K_{d\,11})\lambda_0\lambda_2 + K_{c\,11}\lambda_1^2 + (K_{c\,12} + K_{d\,12})(\lambda_2\zeta_0 + \lambda_0\zeta_2) + 2K_{c\,12}\lambda_1\zeta_1 + (K_{c\,22} + K_{d\,22})\zeta_0\zeta_2 + K_{c\,22}\zeta_1^2 \tag{40}$$

A long-chain hypothesis and quasi-steady-state assumptions are not invoked in deriving the above equations. The quasi-steady-state assumption breaks down when the gel effect sets in, greatly reducing the termination of growing polymer radicals and therefore causing a sudden surge in radical concentration. It is therefore necessary to include eq 32–37 in numerical integration to obtain model predictions. Equations 26–40 are 14 nonlinear ordinary differential equations with the following initial conditions; $I = I_0$, $x = R = \lambda_0 = \lambda_1 = \lambda = \zeta_0 = \zeta_1 = \zeta_2 = \mu_0 = \mu_1 = \mu_2 = 0$, $M_1 = M_{10}$, and $M_2 = M_{20}$. Average molecular weight are calculated from the various moments by the following equations:

$$\bar{M}_n = \frac{(\mu_1 + \lambda_1 + \zeta_1)}{(\mu_0 + \lambda_0 + \zeta_0)} \tag{41}$$

$$\bar{M}_w = \frac{(\mu_2 + \lambda_2 + \zeta_2)}{(\mu_1 + \lambda_1 + \zeta_1)} \tag{42}$$

The polydispersity index is calculated by the ratio of the two average molecular weights as

$$\mathrm{PD} = \frac{\bar{M}_w}{\bar{M}_n} = \frac{(\mu_2 + \lambda_2 + \zeta_2)(\mu_0 + \lambda_0 + \zeta_0)}{(\mu_1 + \lambda_1 + \zeta_1)^2} \tag{43}$$

Equation 43 is often approximated by $\mathrm{PD} = \mu_2\mu_0/\mu_1^2$ in the literature for nongelling systems where a quasi-steady-state approximation is generally invoked.

The instantaneous mole fraction of monomer 1 in copolymer F_1 is obtained from the standard copolymer equation[1-3]

$$F_1 = \frac{r_1 f_1^2 + f_1 f_2}{r_1 f_1^2 + 2 f_1 f_2 + r_2 f_2^2} \tag{44}$$

where r_1 and r_2 are the apparent reactivity ratios, which we develop in the next section, and f_1 and f_2 are the mole fractions of monomers 1 and 2 in the remaining monomer mixture.

Constitutive Equations for the Gel and Glass Effects. Our focus now is to establish a simple algorithm similar to the development by Chiu, Carratt, and Soong[34] (CCS) for the homopolymerization to compute various termination and propagation rate constants over the entire course of reaction. We choose to extend the CCS development because of its model simplicity. Many other theoretical contributions have been made on the subject, among which the work of Cardenas and O'Driscoll,[36] Marten and Hamielec,[32] and Tulig and Tirrell[35] should be particularly mentioned. The latter modeling approaches fit the same set of data by Marten and Hamielec[32] equally well, but each is based on different assumptions. The Marten and Hamielec[32] model, however, has been extended to copolymerization.[30,31,33] However, these models contain parameters which cannot be estimated experimentally.

It is clear termination rate in a thermal copolymer system will depend on the system temperature, chain mobility (thus diffusion), molecular weight of growing radicals, composition of the polymer, and various medium properties. All of the above must be incorporated into the mathematical description underlying the calculation of termination and propagation rate constants. We refer the readers to the CCS paper for detailed derivation of the model and begin here by also following the approach by North.[37] Figures 1 and 2 show an illustrative picture of the termination process with the appropriate coordinate system. Again we will limit our attention to the species of the growing polymer radical pair that eventually terminate each other. The distance r_m is the average minimum separation, within which translational and segmental

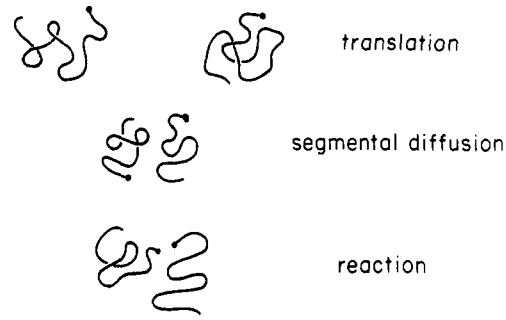

Figure 1. Molecular processes involved in the termination step of free-radical polymerization. Growing radicals are brought together by translational diffusion, whereupon the radical ends reorient by segmental diffusion to facilitate reaction.

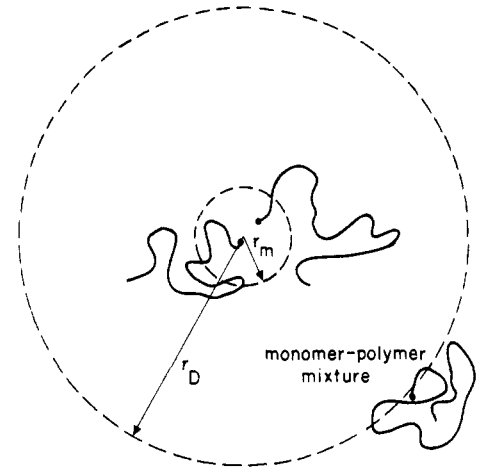

Figure 2. Schematic diagram illustrating the coordinate system used in describing the radical termination process.

diffusion necessary for reaction to occur has been complete. This minimum separation was viewed as the length scale characterizing the effective sphere swept by the free radical end, similar in concept to the Smoluchowski capture radius. For $r \le r_m$, the true termination rate constant, K_{tij}^0, characterizes the ensuing collision process. This true rate constant is an intrinsic parameter, reflecting the rate of reaction under the hypothetical condition unencumbered by diffusion limitations. At a large distance from the radical at the origin, $r \ge r_D$, the concentration of the radical approaches the unperturbed bulk concentration, C_b. The effective concentration C_m for $r \le r_m$ is a function of the radical consumption. In the reaction zone bounded by r_m, the overall rate of radical arrival by diffusion must equal the overall rate of radical termination. The migration of the second radical from $r \gg r_m$ to r_m takes place through diffusion and propagation. Both can be treated as random-walk processes. From CCS and conservation of mass, i.e., the rate of radical transport into a spherical region confined by r_m is equal to the rate of radical consumption in the sphere by termination,

$$4\pi D r_m (C_b - C_m) = \tfrac{4}{3}\pi r_m^3 K_{tij}^0 C_m C_b \tag{45}$$

Here D represents the effective migration coefficient resulting from both diffusive and propagational motion.

The right-hand side of eq 45 is a second-order rate expression that depends on the probability of finding a radical within distance r_m of a central radical, C_m, and the probability of finding the central radical in the system, C_b. Equation 45 can be rearranged to give

$$C_m = \frac{DC_b}{D + (r_m^2/3)K_{tij}^0 C_b} \tag{46}$$

One of the distinguishing features between this model for copolymerization and the CCS model is the way in which the central radical in the system, C_b, is calculated. In homopolymerization the probability the central radical is the radical of interest in the system is one, because there is only one type of radical. The unperturbed bulk concentration is thus C_b. In a copolymer system there exist two types of polymer radicals, one with terminal group M_1 and the other with terminal group M_2. Both polymer radicals can diffuse at the same rate, because the contour-averaged composition of both chains is the same. The only difference is that the terminal groups are not the same. The probability of finding a radical with terminal group M_i among all the radicals can be written as

$$Z_i = P_i/\sum_{i=1}^{N} P_i \tag{47}$$

In a binary copolymerization system, $N = 2$. The probability of finding two radicals with terminal groups M_i is therefore

$$Z_{ii} = P_i^2/(\sum_{i=1}^{N} P_i)^2 \tag{48}$$

Equation 47 does not include the concentration of dead polymers, because those collisions do not result in termination. The unperturbed bulk concentration of central radicals with terminal group M_i is then defined as

$$C_b = P_i Z_i = P_i^2/\sum_{i=1}^{N} P_i \tag{49}$$

Having defined C_b, we have succeeded in expressing the unknown, C_m, in terms of known quantities K_{tij}^0 and D. The overall reaction rate is ordinarily expressed as $K_{tij}C_b^2$, where K_{tij} is the apparent rate constant. This rate is identical with $K_{tij}^0 C_m C_b$, so that we have

$$K_{tij}C_b^2 = K_{tij}^0 C_m C_b \tag{50}$$

Substitution of eq 46 and 48 into eq 50 yields

$$\frac{1}{K_{tij}} = \frac{1}{K_{tij}^0} + (r_m^2/3D)(P_i^2/\sum_{i=1}^{N} P_i) \tag{51}$$

for $i = j$.

For cross-termination reaction rates between growing radicals with terminal groups M_i and M_j, we assume that each is an independent event, and therefore the probability that this will occur sequentially is given by

$$Z_{ij} = Z_i Z_j = P_i P_j/(\sum_{i=1}^{N} P_i)^2 \tag{52a}$$

and similarly

$$Z_{ji} = P_j P_i/(\sum_{i=1}^{N} P_i)^2 \tag{52b}$$

Therefore,

$$\text{the total cross-reaction probability} = 2P_i P_j/(\sum_{i=1}^{N} P_i)^2 \tag{53}$$

The unperturbed bulk concentration for cross-termination reaction is therefore defined as

$$C_b = (\sum_{i=1}^{N} P_i) Z_{ij} = 2P_i P_j/\sum_{i=1}^{N} P_i \tag{54}$$

Comparing the overall reaction rates as before, and separating the terms, we have

$$\frac{1}{K_{tij}} = \frac{1}{K_{tij}^0} + \left(\frac{r_m^2}{3D}\right)\left(\frac{2P_i P_j}{\sum_{i=1}^{N} P_i}\right) \tag{55}$$

for $i \neq j$.

Equations 51–55 are the final constitutive expressions. Note that the overall resistance encountered in chain termination is separated into a reaction-limited and a mass-transfer-limited term. Also note that, D, the effective migration coefficient, is the same in all cases.

We will assume that r_m is a constant, and will be obtained by curve-fitting experimental data. Both K_{tij}^0 and D represent activated processes, and therefore acquire strong temperature dependence. Similar to CCS, K_{tij}^0 lacks the concentration and molecular weight dependence, whereas D assumes a strong dependence on both concentration and molecular weight. Separating D into a temperature and molecular weight dependent front factor, D_0, and a conversion-dependent part, $f(x)$, we have

$$\frac{1}{K_{tij}} = \frac{1}{K_{tij}^0} + \left(\frac{r_m^2}{3D_0}\right)\left(\frac{P_i^2}{\sum_{i=1}^{N} P_i}\right)\frac{1}{f(x)}$$

for $i = j$

$$\frac{1}{K_{tij}} = \frac{1}{K_{tij}^0} + \theta_{tij}\left(\frac{P_i^2}{\sum_{i=1}^{N} P_i}\right)\frac{1}{f(x)} \tag{56}$$

where θ_{tij} ($\equiv r_m^2/3D_0$) has dimensions of time and can be viewed as a characteristic migration time of a growing radical. The case for $i \neq j$ can be similarly treated.

For the glass effect occurring at very high conversions, even diffusion of monomers is impeded. Using an analogous argument, i.e., fixing the radical end at the center and analyzing the diffusion-limited propagation reaction by calculating the effective concentration of the monomer in the vicinity of the growing radical, we obtain the following equation, relating the apparent K_{pij} with the true K_{pij}^0

$$\frac{1}{K_{pij}} = \frac{1}{K_{pij}^0} + \theta_{pij}\frac{P_i}{g(x)} \tag{57}$$

where θ_{pij} is the characteristic monomer diffusion time. Note here for a copolymer system $\theta_{p11} = \theta_{p21}$ and $\theta_{p12} = \theta_{p22}$. The θ_{pij}'s are functions of temperature only and not of the molecular weight of polymer, and $g(x)$ accommodates the conversion dependence of monomer diffusion due to the increasing viscosity of the medium (or decreasing free-volume state of the reaction mixture).

Extension of the Fujita–Doolittle Free-Volume Theory to Copolymerization. In deriving eq 56 and 57, we have not said anything about r_m and D. Here we deal with the significance of such quantities in the context of copolymerization. First, as in CCS we assume r_m to be constant. There is no experimental means at present to determine this otherwise. Second, D is considered a function of radical concentration and molecular weight. Following the Fujita–Doolittle free-volume theory, we adopt its functional dependence during reaction as

$$\ln\frac{D}{D_0} = \frac{\phi_m}{A(T) + B(T)\phi_m} \tag{58}$$

where ϕ_m = volume fraction of total monomers remaining

in the mixture and A and B are functions of temperature. D_0 is the diffusion coefficient in the limit of vanishing ϕ_m, which embodies effects of the initiator concentration and thus the polymer molecular weight.

In a copolymer system the parameters A and B are not available, contrary to the situation for homopolymers. We must therefore develop proper mixing rules for copolymer systems.

Consider a uniform mixture composed of volume V_1 (monomer 1), V_2 (monomer 2), and V_3 of the copolymer. Assuming linear volume additivity, the total volume of the system V is then

$$V = V_1 + V_2 + V_3 \tag{59}$$

Our task is to relate the free-volume state to the system volume, which evolves during reaction. We denote the average free volume in the mixture by V_f and write

$$V_f = V_{fp} + V_{fm} \tag{60}$$

where V_{fp} is the average free volume in the pure polymer at temperature T and V_{fm} is the free volume introduced into the system by the addition of monomers. We assume that the added free volume is a function of T only in the following manner

$$V_f = V_{fp} + \xi(T)(V_1 + V_2) \tag{61}$$

Dividing eq 61 by eq 59 and rearranging give the average free volume fraction f,

$$f = \frac{V_{fp}}{V_3} + \left(\xi(T) - \frac{V_{fp}}{V_3}\right)v_1 + \left(\xi(T) - \frac{V_{fp}}{V_3}\right)v_2 \tag{62}$$

where

$$f \equiv V_f/V \qquad v_1 \equiv V_1/V \qquad v_2 \equiv V_2/V$$

We next define

$$V_{fp}/V_3 \equiv f(T,0,0)$$

and

$$\beta'(T) \equiv \xi(T) - f(T,0,0)$$

Equation 62 can thus be succinctly written as

$$f(T,v_1,v_2) = f(T,0,0) + \beta'(T)(v_1 + v_2) \tag{63}$$

Equations 59–63 provide the basis for estimating the evolving free-volume fraction of a reacting medium. This procedure can be used in conjunction with the Fujita–Doolittle theory for defining D as a function of T and x through calculations of A and B. The functional dependence of D thus predicted can be experimentally assessed by recalling the following relationship, according to Fujita–Doolittle:

$$-\frac{1}{\ln a_c} = f(T,v^*_1,v^*_2) + \frac{[f(T,v^*_1,v^*_2)]^2}{\beta'(T)[(v_1 - v^*_1) + (v_2 + v^*_2)]} \tag{64}$$

where v^*_i is the volume fraction at the reference state and a_c is the viscosity shift factor. In principle, measurement of isothermal viscosity data over a wide composition range allows the free-volume fraction relation derived above to be ascertained. This, in turn, lends support to the predicted functional dependence of D. Such a scenario was indeed followed for homopolymerizing systems as in CCS. However, the lack of adequate viscosity data over a diverse range of composition for copolymer systems necessitates empirical mixing rules to be developed.

Mixing Rules. Let us begin with the following definition:

$$v_{pi} = \frac{\dfrac{M_{i0} - M_i}{\rho_{pi}}}{\left(\sum_{i=1}^{N} \dfrac{M_{i0} - M_i}{\rho_{pi}}\right)} \tag{65}$$

where ρ_{pi} is the density of homopolymer of monomer i. M_{i0} is the initial monomer concentration and M_i is the instantaneous monomer concentration during reaction.

The average free volume in the pure copolymer is defined as

$$B_m = v_{p1}B_1 + (1 - v_{p1})B_2 \tag{66}$$

and

$$A_m = A_1\left(\frac{v_1}{v_1 + v_2}\right) + A_2\left(\frac{v_2}{v_1 + v_2}\right) \tag{67}$$

where A_1, A_2, B_1, and B_2 are parameters for the two-constituent homopolymerization systems.

The Gibbs–DiMarzio equation[38] for the glass transition of a copolymer suggests

$$\ln D_{m_i,0} = \sum_{i=1}^{N} x_i \ln D_{i,0} \tag{68}$$

where $D_{i,0}$ is the homopolymer diffusion coefficient and $D_{m_i,0}$ is the initial diffusion coefficient for the copolymer in the limit of vanishing ϕ_m. Finally, we recognize that the diffusion of polymer radicals will depend on the molecular weight of the growing radicals. Hence,

$$D_{m,0} = D_{m_i,0}(M_w)^{-a} \tag{69}$$

where $D_{m,0}$ is the instantaneous diffusion coefficient for the copolymer radical in the limit of vanishing ϕ_m, $a = 2.0$, from reptation considerations, and M_w is the copolymer molecular weight.

Equations 63–69 are used along with the model eq 26–40. The final equations for the apparent termination and propagation rate constants are then

$$\frac{1}{K_{tij}} = \frac{1}{K_{tij}^0} + \theta_{tij}\left(\frac{P_i^2/\sum_{i=1}^{N} P_i}{\exp\left[\dfrac{\phi_m}{A_m + B_m(T)\phi_m}\right]}\right) \tag{70}$$

for $i = j$, and

$$\frac{1}{K_{pij}} = \frac{1}{K_{pij}^0} + \theta_{pij}\left(\frac{P_i}{\exp\left[\dfrac{\phi_m}{A_j + B_j(T)\phi_m}\right]}\right) \tag{71}$$

and finally

$$\frac{1}{K_{tij}} = \frac{1}{K_{tij}^0} + \theta_{tij}\left(\frac{2P_iP_j/\sum_{i=1}^{N} P_i}{\exp\left[\dfrac{\phi_m}{A_m + B_m(T)\phi_m}\right]}\right) \tag{72}$$

for $i \neq j$, where

$$\theta_{tij} = r_m^2/3D_{m,0} \tag{73}$$

$$\theta_{pij} = r_m^2/3D_{j,0} \tag{74}$$

$$\phi_m = \frac{(1 - x)}{(1 + \epsilon x)} \tag{75}$$

$$B_m = \sum_{i=1}^{N} \upsilon_{pi} B_i \tag{76}$$

$$A_m = \sum_{i=1}^{N} \frac{A_i \upsilon_i}{\sum_{i=1}^{N} \upsilon_i} \tag{77}$$

and

$$\ln D_{m_{i,0}} = \sum_{i=1}^{N} x_i \ln D_{i,0} \tag{78}$$

Numerical solution of the model equations was obtained on a CDC-7600 computer available at the University of California at Berkeley.

The model requires values of several parameters which are experimentally obtainable. The actual values used and their reference sources are given in Tables I–IV.

Results and Discussion

Our primary motivation for this work is to explore procedures for making copolymers with uniform composition. The model serves as a predictive tool to first fit the conversion history data. Once we succeed in doing so we attempt to predict the composition of the copolymer. As a test case, we consider the styrene–methyl methacrylate copolymer system. Experimental composition versus conversion data for this system and homopolymers are available. Since termination by recombination for this monomer pair is not known, we assume only disproportionation.

We begin with the standard *copolymer composition* equation discussed in the introduction.

$$\frac{d[M_1]}{d[M_2]} = \frac{[M_1]}{[M_2]} \frac{r_1[M_1] + [M_2]}{[M_1] + r_2[M_2]} \tag{79}$$

Where $d[M_1]/d[M_2]$ is the ratio of the amount of monomer 1 to monomer 2 that is polymerized during the infinitesimal time dt, i.e., the respective monomer ratios in the copolymer that is produced during this time. The "reactivity ratios" r_1 and r_2 are defined as

$$r_1 \equiv K_p^0{}_{11}/K_p^0{}_{12}$$

and

$$r_2 \equiv K_p^0{}_{22}/K_p^0{}_{21}$$

This equation can be expressed in the form of eq 44 and allows us to construct a polymer composition versus monomer composition plot as shown in Figure 3. We fix $r_1 = 0.007$ and vary r_2 between 0.005 and 100. The series of predicted curves represent the various monomer pairs with the corresponding reactivity ratios. Intersection of each curve with the 45° line represents the azeotrope mole fraction. Ideally in order to produce a uniform composition copolymer, only the azeotrope monomer mole fraction should be used. The system temperature can be altered such that the azeotropic composition matches that desired for the product. However, this may not always be easily accomplished. Any deviation causes the faster reacting monomer to be consumed earlier, until its concentration drops sufficiently, at which point the slower reacting monomer becomes incorporated into the copolymer appreciably. Note that mass-transfer limitations have been totally ignored in Figure 3. As discussed previously the composition "drift" based only on the reactivity differences between the two monomers may only be part of the entire picture. An implicit assumption is made that the rate constants for the various reactions remain constant throughout the course of polymerization. This is obviously a simplification and is the major point of contention concerning the existing literature on copolymerization kinetic models at higher conversion. We hope to complete the picture by accommodating diffusion effects in our kinetic model, shedding some new light possibly on the composition "drift" phenomenon.

We first present the conversion history prediction with our model in the absence of a gel effect (Figure 4). The dashed line is the model prediction and the circles are the

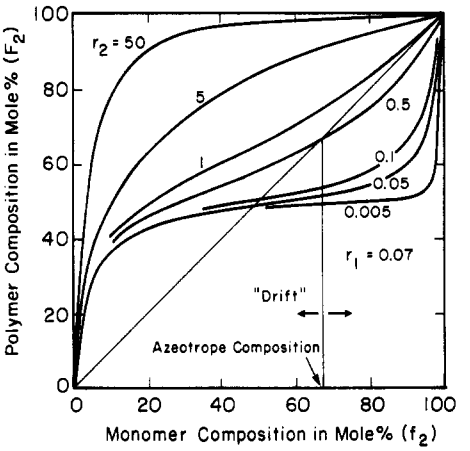

Figure 3. Monomer–polymer composition curves at different intrinsic reactivity ratios. Mass-transfer effects are ignored.

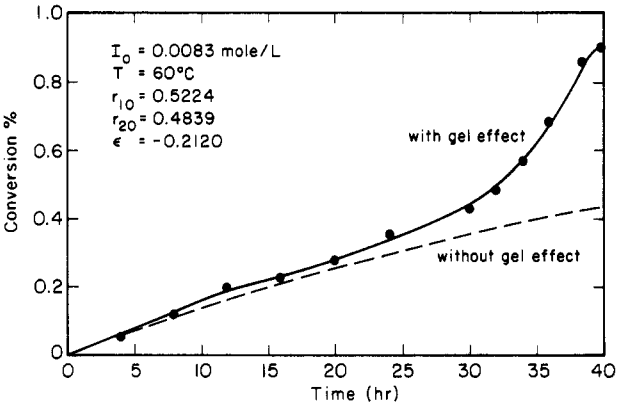

Figure 4. Overall conversion history, for styrene–methyl methacrylate isothermal copolymerization at 60 °C and initiator concentration 0.0083 mol/L. Circles are expreimental data.[24] The dashed curve is predicted by the model without gel effect, whereas the solid curve is with gel effect.

Table I
Numerical Values of Parameters Used in the Model

	Figure			
param	4	5	6	8–12
f	0.58	0.7	0.58	0.8
T_0	338 K	338 K	338 K	338 K
R_{10}^{21}	0.5224 × exp[(−470/R)[(1/T_0) − (1/T)]]			same as 4
R_{20}^{21}	0.4839 × exp[(−566/R)[(1/T_0) − (1/T)]]			same as 4
ϵ	−0.2120	−0.1703[39]	−0.248[39]	−0.2120
ϵ_1	1.0			1.0
ϵ_2	1.0			1.0
w_1	104.14	104.14		104.14
w_2	100.11		100.11	100.11
ρ_1	0.924 − 0.000876(T, °C)	same as 4		same as 4
ρ_2	0.973 − 0.001164(T, °C)		same as 4	same as 4

Table II
Numerical Values of Rate Constants Used in the Model

param	Figure 4	5	6	8–12
$K_D(T)$	$6.982 \times 10^{13} \exp(-29700/RT)$	$1.053 \times 10^5 \exp(-30660/RT)$	same as 5	$6.982 \times 10^{13} \exp(-29700/RT)$
$K_{p}^{0}{}_{11}(T)$, L/(mol s)[21]	$2.790 \times 10^9 \exp(-10620/RT)$	same as 4		same as 4
$K_{p}^{0}{}_{22}(T)$, L/(mol s)[21]	$4.917 \times 10^5 \exp(-4353/RT)$		same as 4	same as 4
$K_{p}^{0}{}_{12}(T)$, L/(mol s)[21]	$2.095 \times 10^7 \exp(-7332/RT)$			same as 4
$K_{p}^{0}{}_{21}(T)$, L/(mol s)[21]	$0.453 \times 10^7 \exp(-5733/RT)$			same as 4
$K_{c}^{0}{}_{11}(T)$, L/(mol s)[21]	$4.839 \times 10^{13} \exp(-8700/RT)$	same as 4		same as 4
$K_{c}^{0}{}_{22}(T)$, L/(mol s)[34]	$9.800 \times 10^7 \exp(-701/RT)$		same as 4	same as 4
ϕ	13			same as 4

Table III
Model Parameters Chosen for Data Fitting

Figure	polym temp, °C	init loading, mol/L	θ_{p11}, min	θ_{p12}, min	θ_{p21}, min	θ_{p22}, min	θ_{t11}, min	θ_{t22}, min	θ_{t12}, min
4	60	0.0083 (Bz_2O_2)							
		without gel effect	0	0	0	0	0	0	0
		with gel effect	6.09×10^4	1.5×10^4	6.09×10^4	1.5×10^4	7.11×10^4	7.11×10^4	7.11×10^4
5	60	0.05 (AIBN)	1.12×10^5	0	0	0	6.0×10^3	0	0
6	60	0.05 (AIBN)	0	0	0	2.76×10^4	0	2.84×10^4	0
8–12	60	0.0083 (Bz_2O_2)	6.09×10^4	1.5×10^4	6.09×10^4	1.5×10^4	7.11×10^4	7.11×10^4	7.11×10^4

Table IV
Model Parameters Chosen for Data Fitting

Figure	polym temp, °C	init loading, mol/L	A_1	A_2	B_1	B_2
4	60 °C	0.0083 (Bz_2O_2)				
		without gel effect	0.085	0.1036	0.025	0.025
		with gel effect	0.085	0.1036	0.025	0.025
5	60 °C	0.05 (AIBN)	0.085		0.02	
6	60 °C	0.05 (AIBN)		0.126		0.03
8–12	60 °C	0.0083 (Bz_2O_2)	0.085	0.1036	0.025	0.025

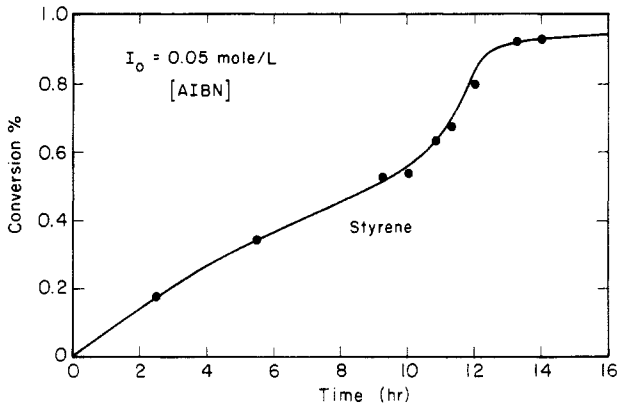

Figure 5. Conversion history, for styrene polymerization at 60 °C, 0.05 mol/L initiator (AIBN) concentration. Circles are experimental data[39] and the solid curve is predicted by the copolymer model.

experimental data[24] for styrene–methyl methacrylate copolymer at 60 °C and initiator loading of 0.0083 mol/L. The particular monomer pair is chosen, as it exhibits a strong gel effect. The model fails badly in fitting the conversion history beyond 25% conversion. Parameter values used to obtain this prediction are listed in Tables I–IV. The refined model with gel and glass effects (eq 26–40 along with the eq 68–78) permits a much better fit, as shown by the solid curve. Model parameters for copolymerization require knowledge of homopolymerization parameters. We follow the CCS approach to first describe homopolymerization reactions. Figures 5 and 6 show excellent fits of data[39] for styrene and MMA homopolymerization, from which several model parameters are determined. The homopolymer model parameters are then used along with our mixing rule to obtain the predicted conversion history curve shown in Figure 7. We could not

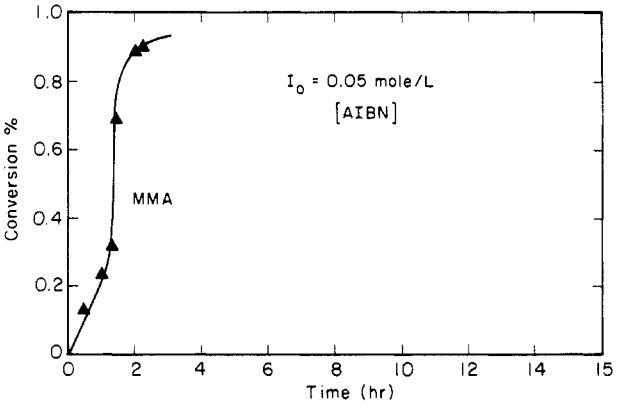

Figure 6. Conversion history, for methyl methacrylate polymerization at 60 °C, 0.05 mol/L initiator (AIBN) concentration. Circles are experimental data[39] and the solid curve is predicted by the copolymer model.

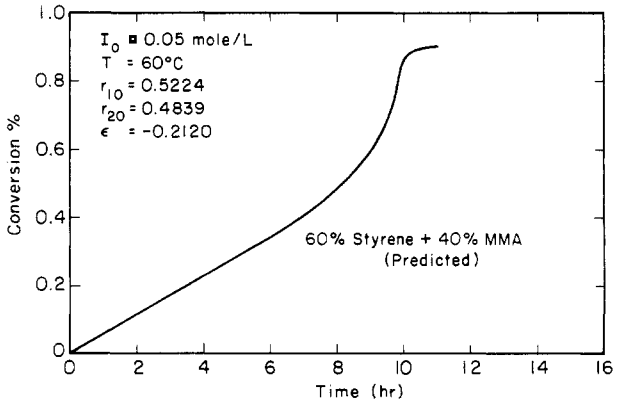

Figure 7. Predicted conversion history for 0.6% styrene–0.4% methyl methacrylate copolymerization at 60 °C and 0.05 mol/L initiator loading.

find any copolymerization experimental data with this initiator loading level in the literature to verify our predicted curve. The parameters are next adjusted for the lower initiator concentration by using the procedure as documented by CCS.

Figure 4 shows the predicted conversion history (solid curve) curve along with the experimental points. The excellent agreement validates our model and the approach used to estimate the parameters. Mass-transfer limitations

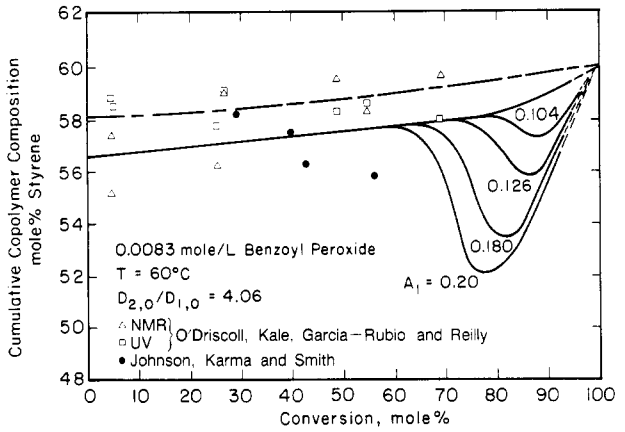

Figure 8. Cumulative copolymer composition versus conversion for 0.6% styrene–0.4% methyl methacrylate copolymer at 60 °C, 0.0083 mol/L (benzoyl peroxide) initiator concentration. $D_{2,0}/D_{1,0}$ = 4.06 for different parameter A_1 values. The points are experimental data,[23,29] and the dot–dash line is fit to O'Driscoll's data[29] by using the Meyer–Lowry equation with r_1 = 0.4971 and r_2 = 0.4639.

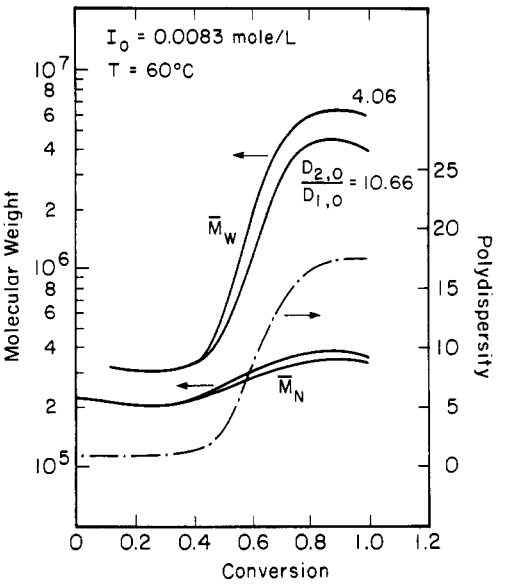

Figure 9. Predicted molecular weight averages and polydispersity as functions of conversion for styrene–methyl methacrylate copolymerization at 60 °C and initiator loading of 0.0083 mol/L.

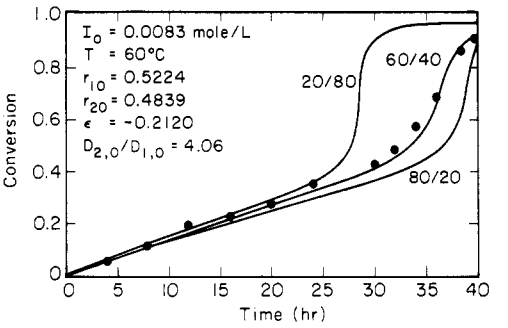

Figure 10. Predicted overall conversion history for styrene–methyl methacrylate copolymerization at 60 °C and initiator loading of 0.0083 mol/L. The circles are experimental data and the solid curves are model predictions for 20/80, 60/40, and 80/20 starting styrene–methyl methacrylate compositions.

are indeed important. The model can now be employed for predicting cumulative copolymer composition versus conversion (Figure 8). For the styrene–methyl methacrylate monomer pair at 60 °C and 0.0083 mol/L initiator concentration, several curves are obtained by changing the parameter which affects the diffusion coefficient ratio of the two monomers. The predicted composition curves show increasing drifts in the copolymer composition as the apparent diffusion coefficient ratio of monomer 2 over monomer 1 increases. Note that in order for the *cumulative* composition to drift noticeably, the instantaneous composition must deviate significantly from that produced up to the moment. As a result, the composition distribution becomes correspondingly broad. This considerably changes the engineering properties of the product.

Figure 8 also shows the experimental data by Johnson et al.[23] and O'Driscoll et al.[29] O'Driscoll's new data do not show the same large composition drift as Johnson et al., although the data are only limited to 70 wt % conversion. Due to the limited range of experimental data available, it is not possible to determine conclusively if diffusion effects are operative on the respective propagation reactions. Our model predictions consistently give a slightly lower cumulative copolymer composition in comparison with the Meyer–Lowry prediction. This discrepancy is due to the different intrinsic kinetic parameters chosen in our calculations. We did not attempt to optimize the parameters to achieve agreement with the Meyer–Lowry equation, because it is not critical for the subsequent discussions.

Note that if the mass-transfer limitation on the propagation rate constants in the glass effect region exists, composition drifts are predicted at higher conversions. The experimental data at present do not allow us to resolve the mass-transfer effect on the composition. However, our predictions nevertheless suggest large composition drifts in case the apparent reaction rate constants change at high conversions (>70%). We believe more experimental work at such conversion levels is needed.

It is our intention to test our model predictions against experimental data available on other copolymers.[30,31,33] For methyl methacrylate–*p*-methylstyrene copolymer, Jones et al.[31] tested the hypothesis of reactivity change with conversion by solving the differential form of the Meyer–Lowry equation with r_1 and r_2 changing with conversion. Again their conclusion was that the available data were not of sufficient accuracy to verify or disprove the hypothesis.

An interesting feature has been brought to light which has hitherto not been addressed. Since a large fraction of monomers react upon the onset of gel effect, major detrimental effect on the copolymer properties may be induced by this later-stage composition "drift". Although the effect on propagation rate in the gel effect region may not be very strong, the region between gel and glass effect would likely witness significant monomer diffusion limitations.

Figure 9 shows model predictions for the weight- and number-average molecular weights, at two different apparent diffusion coefficient ratios. No experimental data at the above conditions is available. Also shown is the polydispersity curve. A 10-fold molecular weight increase is encountered during the gel effect, which is consistent with the experimentally observed and predicted data for methyl methacrylate–*p*-methylstyrene copolymer.[31]

Finally, Figures 10 and 11 further demonstrate model predictions of the conversion history and cumulative copolymer composition versus conversion, for the styrene–methyl methacrylate monomer pair at 20/80, 60/40, and 80/20 starting compositions at 60 °C. As expected, the larger the amount of the methyl methacrylate monomer (gel effect enhancer), the greater the possible copolymer composition drifts. Conversely, predominance of styrene in the monomer mix reduces composition drifts.

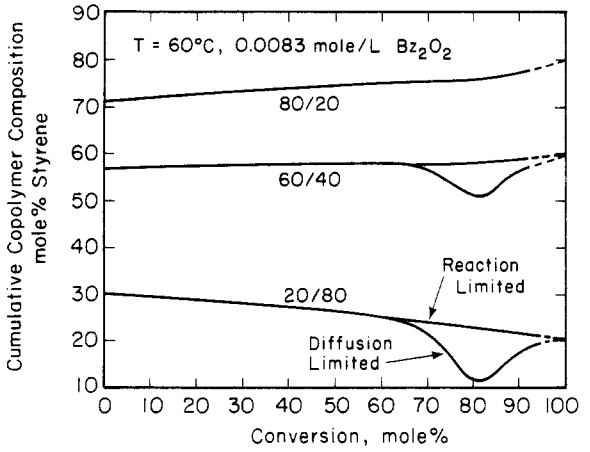

Figure 11. Predicted cumulative copolymer composition (mol % styrene) versus overall conversion, at 60 °C and initiator loading of 0.0083 mol/L. The solid curves are predictions for 20/80, 60/40, and 80/20 starting monomer styrene–methyl methacrylate compositions.

We summarize the important observations of this paper as follows: (a) Diffusion limitation during polymerization may cause considerable composition "drift", possibly in regions near the glass effect, over and above that attributable to intrinsic reactivity mismatch. (b) Molecular weight increase of 10–20-fold is common in the gel effect region. (c) Our copolymerization model can correctly predict the conversion history and the cumulative composition trends, once diffusional limitations are incorporated. (d) Any optimum strategy for controlling the copolymer composition must consider the mass-transfer limitations during the reaction. The experimentally determined reactivity ratios at low levels of conversion may not be used without modification for copolymer modeling at higher conversions.

Many fundamental questions remain. For example, the discrepancy at high conversions between data and theory should be resolved. In addition, heat-transfer effects which are neglected by assuming isothermal conditions (good mixing) require validation. Considerable heat of reaction is liberated during the polymerization, therefore does the experimental system truly maintain a constant temperature? Knowing that heat- and mass-transfer limitations exist, what control strategies are superior for obtaining uniform composition? Is constant composition always desirable?

These questions, and many others, await future progress in the field of copolymerization reaction engineering. As noted earlier, the comparison of model predictions against experimental data on other copolymers will be undertaken in the next paper, once the individual monomer conversion history is available.

Acknowledgment. D. Sharma acknowledges the Dow Chemical Co. for providing an excellent research environment, where this work was conceived. Constructive suggestions by Dr. Mike Mintz, Marv McDonald, and Dr. Jim Pierce at Dow Chemical Co. are gratefully acknowledged.

Registry No. (Styrene)(methyl methacrylate) (copolymer), 25034-86-0.

References and Notes

(1) Alfrey, T.; Goldfinger, G. *J. Chem. Phys.* **1944**, *12*, 205.
(2) Mayo, F. R.; Lewis, F. M. *J. Am. Chem. Soc.* **1944**, *66*, 1594.
(3) Wall, F. T. *J. Am. Chem. Soc.* **1944**, *66*, 2050.
(4) Skiest, I. *J. Am. Chem. Soc.* **1946**, *68*, 1781.
(5) Mayo, F. R.; Walling, C. *Chem. Rev.* **1950**, *46*, 191.
(6) Ham, G. E. In *High Polymer Series*; Wiley: New York, 1964; Vol. XVIII.
(7) Meyer, V. E.; Lowry, G. G. *J. Polym. Sci., Part A* **1965**, *3*, 2843.
(8) Hanson, A. W.; Zimmerman, R. L. *Ind. Eng. Chem.* **1957**, *49*, 1803.
(9) Hanna, R. J. *Ind. Eng. Chem.* **1957**, *49*, 208.
(10) O'Driscoll, K. F.; Knorr, R. *Macromolecules* **1968**, *1*, 367.
(11) O'Driscoll, K. F.; Knorr, R. *Macromolecules* **1969**, *2*, 507.
(12) Szabo, T. T.; Nauman, E. B. *AIChE J.* **1969**, *15*, 575.
(13) Ray, W. H.; Gall, C. E. *Macromolecules* **1969**, *2*, 425.
(14) Ray, W. H. *J. Macromol. Sci.—Rev. Macromol. Chem.* **1972**, *C8* (1), 1.
(15) Macklenburg, J. C. *Can. J. Chem. Eng.* **1970**, *48*, 279.
(16) Tirrell, M.; Gromley, K. *Chem. Eng. Sci.* **1981**, *36*, 367.
(17) Ray, W. H.; Szekely, J. In *Process Optimization* Wiley: New York, 1973.
(18) Tsoukas, A.; Tirrell, M.; Stephanopoulos, G. *Chem. Eng. Sci.* **1982**, *37*, 1785.
(19) Guyot, A.; Guillot, J.; Pichot, C.; Guerrero, L. R. *ACS Symp. Ser.* **1981**, *No. 165*, 415.
(20) Garcia-Rejon, A.; Guzman, C.; Mendez, J. C.; Rios, L. *Chem. Eng. Commun.* **1983**, *24*, 71.
(21) Meyer, V. E. *J. Polym. Sci., Polym. Chem. Ed.* **1967**, *5*, 1289.
(22) Chan, R. K. S.; Meyer, V. E. *J. Polym. Sci., Part C* **1968**, *25*, 11.
(23) Johnson, M.; Karma, T. S.; Smith, R. R. *Eng. Polym. J.* **1978**, *14*, 409.
(24) Dionisio, J. M.; O'Driscoll, K. F. *J. Polym. Sci., Polym. Lett.* **1979**, *17*, 701.
(25) Teramachi, S.; Hasegawa, A.; Uchiyama, N. *J. Polym. Sci., Polym. Lett. Ed.* **1984**, *22*, 71.
(26) Inagaki, H.; Matsuda, H.; Kamiyama, F. *Macromolecules* **1968**, *1*, 520.
(27) Teramachi, S.; Hasegawa, A.; Yoshida, S. *Polym. J.* **1982**, *14*, 161.
(28) Inagaki, H. In *Fractionation of Synthetic Polymers*; Tung, L. H., Ed.; 1977, Marcel Dekker: New York; Chapter 7.
(29) O'Driscoll, K. F.; Kale, L. T.; Garcia-Rubio, L. H.; Reilly, P. M. *J. Polym. Sci., Polym. Chem. Ed.* **1984**, *22*, 2777.
(30) Garcia-Rubio, L. H.; Lord, M. G.; MacGregor, J. F.; Hamielec, A. E. *Polymer* **1985**, *26*, 2001.
(31) Jones, K. M.; Bhattacharya, D.; Brash, J. L.; Hamielec, A. E. *Polymer* **1986**, *27*, 602.
(32) Marten, F. L.; Hamielec, A. E. *ACS Symp. Ser.* **1979**, *No. 104*, 43.
(33) Bhattacharya, D.; Hamielec, A. E. *Polymer* **1986**, *27*, 611.
(34) Chiu, W. Y.; Carratt, G. M.; Soong, D. S. *Macromolecules* **1983**, *16*, 348.
(35) Tulig, T. J.; Tirrell, M. *Macromolecules* **1981**, *14*, 1501.
(36) Cardenas, J. N.; O'Driscoll, K. F. *J. Polym. Sci.* **1976**, *14*, 883.
(37) North, A. M. In *The Collision Theory of Chemical Reactions in Liquids*; Wiley: New York, 1964.
(38) Gibbs, J. H.; DiMarzio, E. A. *J. Chem. Phys.* **1958**, *28*, 373.
(39) Nishimura, N. *J. Macromol. Chem.* **1966**, *2*, 259.